

VALIDATION OF MODELS FOR THE DIFFUSION WEIGHTED MR SIGNAL IN BRAIN WHITE MATTER

Els Fieremans¹, Yves De Deene^{1,2} and Ignace Lemahieu¹

¹ Department of Electronics and Information Systems, MEDISIP, Ghent University-IBBT-IBiTech,

² Department of Radiotherapy and Nuclear Medicine, QMRI, Ghent University Hospital, De Pintelaan 185 block B, B-9000 Belgium

ABSTRACT

The diffusion weighted MR-signal attenuation in brain white matter is not mono-exponential. A bi-exponential model has been proposed since this fits the data well. We have modeled the diffusion weighted MR-signal by Monte Carlo simulations in a fiber geometry similar to brain white matter. Although the bi-exponential model fitted the data very well, the fitted diffusion coefficients and fractions did not converge to the simulated values in the intra and extra cellular space. However, fitting the cumulant expansion form terminated after the N^{th} order term to the data results in accurate fits for the diffusion coefficient and kurtosis.

Index Terms— Biomedical magnetic resonance imaging, Diffusion processes, Brain modeling, Monte Carlo methods

1. INTRODUCTION

Diffusion weighted magnetic resonance imaging (DW-MRI) provides a non-invasive tool to explore fibrous tissue *in vivo*. An interesting application for DW-MRI is the investigation of brain white matter where the insight in the anatomy of neuronal networks is of great interest for the understanding of normal and pathological processes affecting brain functions (for an overview see [1]).

In brain white matter, barriers of axonal membranes and myelin sheets are responsible for anisotropic diffusion. The diffusion is restricted and the DW-MRI signal as a function of the b-factor can not be described accurately by a mono-exponential function. Numerous studies [1] suggest that the DW-MRI signal in brain white matter can be described by a bi-exponential model, i.e. a weighted sum of two exponential functions, since this model fits the data very well. Although it was suggested that these two pools would correspond with the intra and extra cellular water pools, the corresponding fractions do not agree with the fractions known for the intra and extra cellular space [1]. In addition, these compartments have not been histologically identified neither [2].

Thanks to the IWT for funding.

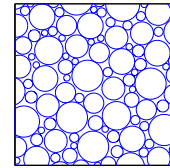


Fig. 1. A cross-section of $80 \mu\text{m} \times 80 \mu\text{m}$ through the generated phantom consisting of parallel cylinders, showing the random packing geometry and the variation in diameter of the cylinders.

In this study, Monte Carlo simulations were performed in a fiber geometry similar to those observed in brain white matter. The bi-exponential model has been evaluated as a function of the considered b-interval. In addition, the cumulant expansion form has been tested, whereby the logarithm of the DW-MRI signal is developed as a power series of b.

2. METHODS

2.1. Simulations

2.1.1. Phantom Generation

The diffusion process was modeled in a raster consisting of infinitely long parallel aligned rigid cylinders with a square cross-section of $1 \text{ mm} \times 1 \text{ mm}$. The diameters and the density of the cylinder packing were chosen similar to those observed in brain white matter [1]. The radii of the cylinders were generated according to a Gaussian distribution with a mean radius of $5 \mu\text{m}$ and a standard deviation of $1.75 \mu\text{m}$. The density of the cylinder packing was 79.5%. Fig. 1 shows a cross-section of the cylinder packing.

2.1.2. Random walk simulation

The diffusion process was modeled by Monte Carlo simulation of random walkers. 300.000 particles were initially randomly spread in the raster. The trajectory of one spin particle

was generated by moving the particle during each time step t over a distance of $\sqrt{6D_{\text{free}}t}$ (with D_{free} the diffusion coefficient of water in a free medium) in a randomly chosen radial direction. There is no exchange between the inside and outside of the cylinders, so at the cylinder boundaries, particles were elastically reflected. In the direction along the cylinders, the particles can travel infinitely long. In the transverse direction, random walkers that reach one side of the $1 \text{ mm} \times 1 \text{ mm}$ square, re-enter again at the opposite side of the square. For each random walker, the number of times that it leaves and enters the square at each side is recorded so that for a given diffusion time Δ , the total traveled distance could be calculated correctly. The first and higher order moments of the total traveled distance in the direction perpendicular and parallel to the fibers are used to calculate the apparent diffusion coefficient D_{app} and the apparent diffusion kurtosis K_{app} according to the corresponding definitions:

$$D_{\text{app}}(\Delta) = \frac{1}{2\Delta} \left\langle (\vec{n} \cdot \vec{s})^2 \right\rangle \quad (1)$$

$$K(\Delta) = \frac{\left\langle (\vec{n} \cdot \vec{s})^4 \right\rangle}{\left\langle (\vec{n} \cdot \vec{s})^2 \right\rangle^2} - 3 \quad (2)$$

where \vec{s} is the net displacement of a particle during a diffusion time Δ in a given direction \vec{n} .

Kurtosis is a measure of peakedness of a distribution. The kurtosis equals zero in case of Gaussian diffusion and becomes positive if the diffusion probability function is less sharply peaked than a Gaussian distribution.

When applying a diffusion gradient \vec{G} during a time δ , the phase ϕ of the spin particles was updated during each time step dt by:

$$\Delta\phi = \gamma \cdot \vec{G} \cdot \vec{r} \cdot dt$$

where γ is the gyro magnetic ratio, \vec{r} is the position of the spin and

$$\vec{G} = \begin{cases} G \cdot \vec{n} & \text{if } 0 < t \leq \delta \\ -G \cdot \vec{n} & \text{if } \Delta < t \leq \Delta + \delta \\ 0 & \text{at other times} \end{cases}$$

The diffusion weighted MR-signal was then derived as the sum of the phases of all spins: $\sum e^{i\phi}$. For all calculations and fittings, the magnitude of this signal will be used, denoted as S .

The diffusion gradient is chosen perpendicular to the fibers. Varying diffusion gradients were applied during a time δ of 0.7 ms. Increasing diffusion times Δ (2 ms up to 100 ms) were considered so that the corresponding b-factors, defined by $\gamma^2 \delta^2 G^2 (\Delta - \delta/3)$, ranged from 0 up to 10.000 s/mm^2 . The diffusion coefficients for a free medium were chosen similar to those described in literature for the intra and extra cellular

space of brain white matter [3]: $10^{-9} \text{ m}^2/\text{s}$ inside the cylinders and $2.5 \cdot 10^{-9} \text{ m}^2/\text{s}$ outside the cylinders.

The diffusion process and the DW-MRI signal have been simulated inside and outside of the cylinders simultaneously to obtain D_{app} and K_{app} and $S(b)$. In addition, the diffusion process has been simulated separately inside the cylinders and outside the cylinders to obtain the corresponding apparent diffusion coefficients D_{in} and D_{ex} .

Simulations were performed for 300.000 spins with a time-step dt of 0.07 ms. The accuracy of the simulation of D_{app} and K_{app} has been addressed previously [4]. The accuracy of the simulation of the DW-MRI signal S was addressed by simulating the diffusion weighted MR signal in a free medium, showing an exponential decay of S as a function of b according to $S = e^{-bD_{\text{free}}}$.

2.2. Data fitting

The validity of the bi-exponential model was tested by fitting the following function to the simulated $S(b)/S(b=0)$ -curve for each diffusion time Δ using a Levenberg-Marquard algorithm:

$$\frac{S(b)}{S(0)} = \alpha e^{-bD_{\text{slow}}} + (1 - \alpha) e^{-bD_{\text{fast}}} \quad (3)$$

The fitted values for α , D_{slow} and D_{fast} were compared to the theoretical value for $\alpha = 0.80$ and the simulated values for the diffusion coefficient inside the cylinders and outside the cylinders D_{in} and D_{ex} .

In addition, a model independent description for S has been investigated where the logarithm of S is fitted as a power series in b [5]:

$$\ln\left(\frac{S(b)}{S(0)}\right) = C_1 \cdot b + C_2 \cdot b^2 + C_3 \cdot b^3 + \dots \quad (4)$$

This formula describes the cumulant expansion of $\ln S$ in powers of the applied gradients. The coefficients of the first and second order yield the apparent diffusion coefficient D_{app} and kurtosis K_{app} :

$$C_1 = -D_{\text{app}} \quad (5)$$

$$C_2 = \frac{1}{6} K_{\text{app}} D_{\text{app}}^2 \quad (6)$$

The termination of the series in eq.(4) after the N^{th} order term is called the b^N cumulant expansion form. The usefulness of the cumulant expansion form to describe the diffusion weighted signal attenuation depends crucially on its convergence. We have investigated this by fitting polynomials of the order $N = 1$ up to 10 to the logarithm of $S(b)$ for each diffusion time Δ . For every fitted b^N cumulant form, the fitted coefficients corresponding to the first and second order were used to obtain D_{app} and K_{app} using eq. (5) and eq. (6). The fitted values were then compared to the simulated values D_{app} and K_{app} obtained from the diffusion simulations.

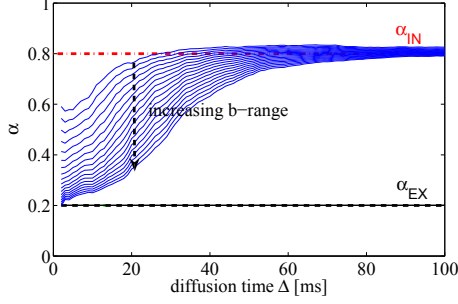


Fig. 2. Bi-exponential fitting results (eq. (3)) for α as a function of the diffusion time Δ . α , the fraction corresponding to the slowest apparent diffusion coefficient (D_{slow} in eq. (3)) is compared to the theoretical fraction of the cylinder packing (α_{in} - dotted red line) and the fraction outside the cylinders (α_{ex} - dotted black line). The fitted α -values depend on the considered b -interval: [0-1500 s/mm²] up to [0-10000 s/mm²].

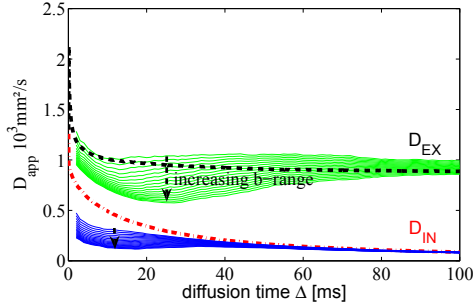


Fig. 3. Bi-exponential fitting results (eq. (3)) for D_{fast} and D_{slow} as a function of the diffusion time Δ . D_{slow} and D_{fast} are compared to the theoretical values for D_{app} inside the cylinders (D_{in} - dotted red line) and outside the cylinders (D_{ex} - dotted black line). The fitting results depend on the considered b -interval: ([0-500 s/mm²] up to [0-10000 s/mm²]).

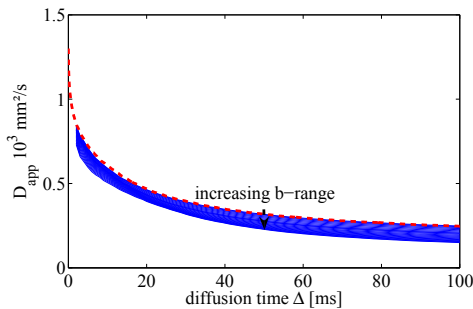


Fig. 4. Fitting results of D_{app} using the b^2 cumulant expansion (eq. (4)) in comparison to the simulated value (dotted line). When increasing the considered b -interval for the fit from [0-500 s/mm²] up to [0-10000 s/mm²], the difference between fitted and theoretical D_{app} -values increases.

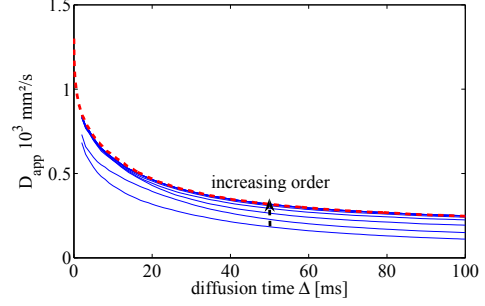


Fig. 5. Fitting results of D_{app} using the cumulant expansion (eq. (4)) b^N for increasing order ($N=1$ up to 10) and a fixed b -interval of [0-10000 s/mm²] in comparison to the simulated value (dotted line). Incorporating higher order terms of the cumulant expansion results in a slightly better agreement between fitted and theoretical values for D_{app} .

3. RESULTS

For all diffusion times Δ , the datasets $S(b)$ could be fitted to the bi-exponential model, eq. (3), with a correlation coefficient of minimum 0.9999. Fig. 2 shows the fitted values for α as a function of Δ considering increasing b -intervals. α is the fraction corresponding with the slowest D_{app} and should be equal to the water fraction inside the cylinders, i.e. 0.8. For long diffusion times, the best agreement between theoretical and fitted values of α is obtained. When including a large b -interval in the fit, the water fraction inside the cylinders is underestimated, especially at short diffusion times. Fig. 3 presents the fitted values for D_{fast} and D_{slow} as a function of Δ considering increasing b -intervals. D_{slow} corresponds with the fitted fraction α and should thus be compared to D_{in} while D_{fast} should be compared to D_{ex} . The best agreement is obtained at long diffusion times. When including a large b -interval in the fit, D_{fast} and D_{slow} are underestimated, especially at short diffusion times.

For all diffusion times Δ , the datasets $S(b)$ were fitted to the cumulant expansion b^N (eq. (4)). The fitted D_{app} - and K_{app} -values were then compared to their simulated values. For D_{app} , fig. 4 shows the dependency on the considered b -interval and fig. 5 shows the dependency on the order N of the cumulant expansion. Similar plots are shown for K_{app} in fig. 6 and fig. 7. The cumulant expansion fits of $S(b)$ with the highest correlation coefficients resulted in fitted values for D_{app} and K_{app} which were closest to the simulated values. The minimum order N to obtain a good agreement between fitted and simulated values for D_{app} and K_{app} decreases when decreasing the b -interval of the fit. When $N \geq 7$, the fitted values for D_{app} and K_{app} equal the simulated values for all considered b -ranges. Cumulant expansion forms with $N = 3$ result in accurate fits for D_{app} and K_{app} for b -intervals ranging up to 2500 s/mm².

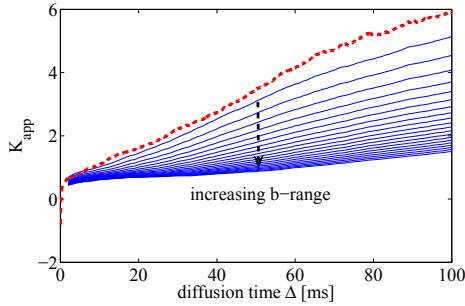


Fig. 6. Fitting results of K_{app} using the b^2 cumulant expansion (eq. (4)) in comparison to the simulated value (dotted line). When increasing the considered b -interval for the fit from $[0 - 500 \text{ s/mm}^2]$ up to $[0 - 10000 \text{ s/mm}^2]$, the difference between fitted and theoretical K_{app} -values increases.

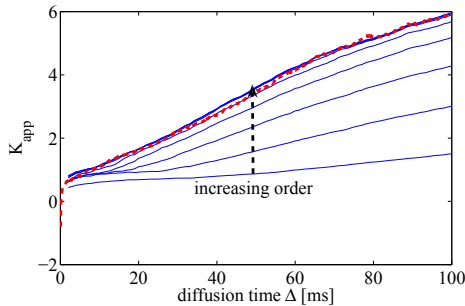


Fig. 7. Fitting results of K_{app} using the cumulant expansion (eq. (4)) b^N for increasing order ($N=2$ up to 10) and a fixed b -interval of $[0 - 10000 \text{ s/mm}^2]$ in comparison to the simulated value (dotted line). Incorporating higher order terms of the cumulant expansion results in a considerably better agreement between fitted and theoretical values for K_{app} .

4. DISCUSSION

As can be derived from fig. 2 and fig. 3, the fitting results of D_{in} , D_{ex} and α are dependent on the employed b_{max} and the diffusion time. Moreover, the fitted values for α differ from the real water fraction inside the cylinders at short diffusion times. This indicates that the fitted fractions and corresponding diffusion coefficients do not stand for the diffusion inside and outside the cylinders. Furthermore, pseudo bi-exponential diffusion weighted signal attenuation can be observed in single compartment systems such as the intra cellular space [3] and the interstitial space between fibers [4]. The good quality of fitting a bi-exponential function to the data is not sufficient to prove the accuracy of this model. The results in this study suggest that the signal attenuation curve is not truly bi-exponential.

This study proves the convergence of the cumulant expansion form when fitting the diffusion weighted signal at-

tenuation. The results of fig. 4, fig. 5, fig. 6 and fig. 7 show that D_{app} and K_{app} could be accurately fitted if the order N is large enough in relation to the considered b -interval. The cumulant expansion form might be an alternative to the bi-exponential model to fit the diffusion weighted MR signal in b -intervals in the range of $[0 - 2500 \text{ s/mm}^2]$. Particularly in case of exchange between the intra cellular and extra cellular space, the bi-exponential model, based on a two-compartment system, is not straightforward interpretable. The kurtosis may be a useful parameter then to estimate the permeability [5].

Preliminary measurements reveal that fitting the cumulant expansion form is more robust against noise than fitting the bi-exponential model. When using the cumulant expansion form b^N , the precision of D_{app} and K_{app} decreases while the accuracy increases with N . Further research will focus on finding the optimal N for a given dataset and noise level.

5. CONCLUSION

The diffusion weighted MR signal has been simulated in a fiber geometry similar to brain white matter tissue. The bi-exponential model for the signal attenuation curve has been evaluated. The good accuracy of the bi-exponential fit does not prove the validity of the model since there is a strong dependence on the considered b -interval and diffusion time. The cumulant expansion form is proposed as a useful alternative. When including higher order terms the diffusion coefficient and kurtosis could be accurately fitted.

6. REFERENCES

- [1] D. Le Bihan, "The 'wet mind': water and functional neuroimaging," *Phys. Med. Biol.*, vol. 52, no. 7, pp. 57–90, April 2007.
- [2] Valerij G. Kiselev and Kamil A. Il'yasov, "Is the "biexponential diffusion" biexponential?," *Magnetic Resonance in Medicine*, vol. 57, no. 3, pp. 464–469, 2007.
- [3] Y. Assaf, R. Z. Freidlin, G. K. Rohde, and P. J. Basser, "New modeling and experimental framework to characterize hindered and restricted water diffusion in brain white matter.," *Magn Reson Med*, vol. 52, no. 5, pp. 965–978, November 2004.
- [4] E. Fieremans, Y. De Deene, S. Delpitte, M.S. Ozdemir, Y. D'Asseler, J. Vlassenbroeck, K. Deblaere, E. Achten, and I. Lemahieu, "Simulation and experimental verification of the diffusion in an anisotropic fiber phantom.," *J Magn Reson*, vol. 190, no. 2, pp. 189–199, Februari 2008.
- [5] J. H. Jensen, J. A. Helpert, A. Ramani, H. Lu, and K. Kaczynski, "Diffusional kurtosis imaging: the quantification of non-gaussian water diffusion by means of magnetic resonance imaging," *Magn. Reson. Med.*, vol. 53, no. 6, pp. 1432–1440, June 2005.